Effective viscosity of glycerin in a nanoporous silica gel

Aijie Han,[1] Weiyi Lu,[1] Venkata K. Punyamurtula,[1] Xi Chen,[2] Falgun B. Surani,[3] Taewan Kim,[4] and Yu Qiao[1,4,a)]
[1]*Department of Structural Engineering, University of California–San Diego, La Jolla, California 92093-0085, USA*
[2]*Department of Civil Engineering and Engineering Mechanics, Columbia University, New York, New York 10027, USA*
[3]*Department of Civil Engineering, University of Akron, Akron, Ohio 44325, USA*
[4]*Program of Materials Science and Engineering, University of California–San Diego, La Jolla, California 92093, USA*

(Received 15 January 2008; accepted 26 September 2008; published online 30 December 2008)

The infiltration of glycerin in a lyophobic nanoporous silica gel is investigated experimentally, and the effective interfacial tension and viscosity are discussed. While the simple superposition principle can be employed for the analysis of interfacial tension, in a nanopore the effective liquid viscosity is no longer a material constant. It is highly dependent on the pore size and the loading rate, much smaller than its bulk counterpart. © *2008 American Institute of Physics*. [DOI: 10.1063/1.3020535]

I. INTRODUCTION

The study on nanofluidic behaviors has provided a solid basis for understanding solid-liquid interactions in nanoenvironments.[1,2] Through molecular dynamics simulations, it was predicted that in a nanochannel liquid molecules can form a one dimensional chainlike structure, and their transportation can be "frictionless," [3–6] primarily because at the nanometer level the ordinary shearing and flowing processes break down. Recently, a few experimental studies have been carried out to develop "superdashpots" using nanoporous materials.[7,8] As a liquid infiltrates in a nanoporous material, the large nanopore surface can greatly amplify the solid-liquid interaction, and therefore the system becomes a high-performance damper.[9–12] For instance, Li[9] analyzed the damping properties of a hydrophilic nanoporous silica plate soaked by water. As a bending moment was applied on the plate, water moved from compressive parts to tensile parts and thus a certain amount of energy was dissipated. The energy dissipation efficiency, which was measured by the amount of energy absorbed by a unit mass of material, however, was lower than the expected level, indicating that in the nanopores the effective liquid viscosity was smaller than that of the bulk phase.

In another set of experiments, Kong and Qiao[13] reported that the capillary effect of nanoporous materials is more controllable. By applying a nominally hydrostatic pressure on a system containing a hydrophobic nanoporous silica gel immersed in water, as the pressure was sufficiently high the liquid phase could be forced into the nanopores. It is remarkable that as the loading rate increased, in a Hopkinson bar arrangement of impact test,[14] the energy absorption efficiency was increased by nearly two times. Since the excess solid-liquid interfacial tension should be rate independent, the increase in energy dissipation capacity was attributed to the liquid viscosity. It is thus envisioned that if more viscous liquids, such as glycerin, are employed, the rate dependence of energy absorption can be promoted.

II. EXPERIMENTAL

In the current study, we investigated pressure induced infiltration of a hydrophobic Fluka 100 C_8 reversed phase silica gel synthesized through a sol-gel templating technique. The material was in powder form, with the particle size of 15–35 μm. The nanopore surfaces were treated by silane groups, so that they were highly hydrophobic.[15] Through a gas absorption test, it was measured that the particles contained 0.55 cm^3/g of nanopores, with the average pore size of 7.8 nm and the standard deviation of 2.4 nm. The liquid phase was chosen as Aldrich 7757 glycerin ($C_3H_8O_3$). Its molecular weight was 92.09, the molecular size was about 0.3 nm, and the viscosity was 1.5 Pa s. It was stored in a drying hood so as to minimize the exposure to moisture.[16] The polarity of glycerin molecule is quite high, and therefore it can be easily mixed with water and is nonwetting to the nanopore surface. Its viscosity is higher than that of water by more than two orders of magnitude. Due to the small molecular size, when subjected to a high pressure, glycerin molecules were able to enter most of the nanopores in the silica gel.

After mixing 0.5 g of the nanoporous silica gel with 7 g of aqueous solution of glycerin in a stainless steel cylinder, the cylinder was sealed by a stainless steel piston. By using a type 5569 Instron machine, the piston was compressed into the cylinder at a constant rate in the range of 1–90 mm/min. When the pressure reached about 50 MPa, the crosshead was moved back at the same speed. Figure 1 shows typical sorption isotherm curves of samples of various glycerin concentrations at the loading rate of 1 mm/min. The glycerin concentration, c, varied from 0 (pure water) to 100 wt % (pure glycerin). Figure 2 shows the sorption isotherm curves of pure glycerin based systems at various loading rates. The pressure was calculated as $P=F/A_0$, with F being the force

a)Author to whom correspondence should be addressed. FAX: +1-330-972-6020. Electronic mail: yqiao@ucsd.edu.

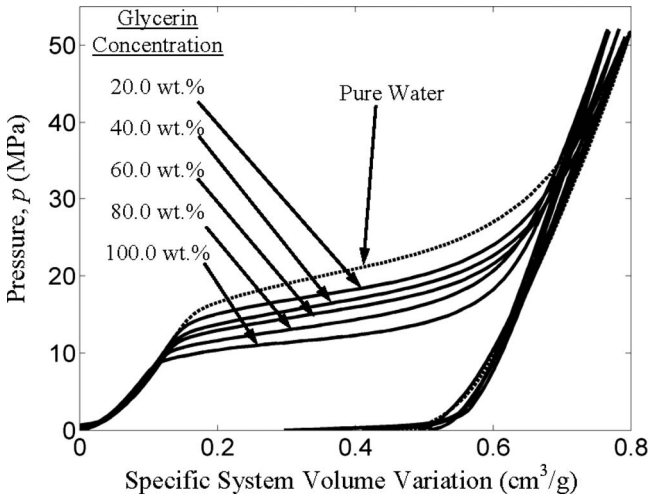

FIG. 1. The sorption isotherm curves of systems of various glycerin concentrations. The loading rate was 1 mm/min.

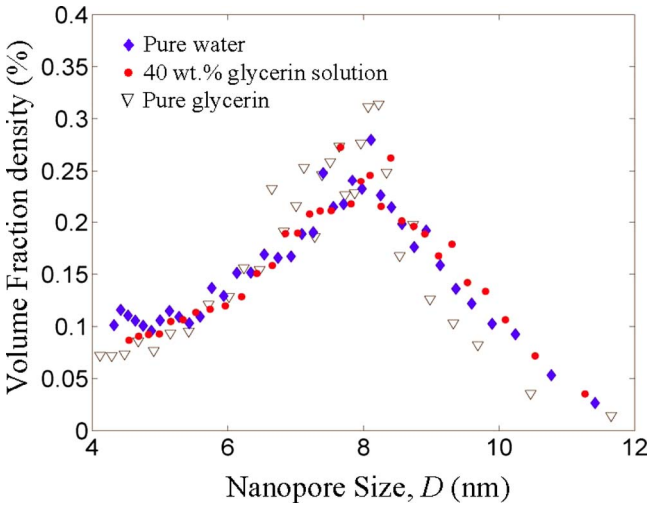

FIG. 3. (Color online) The pore size distribution curves.

applied on the piston and A_0 the cross-sectional area of the piston. The specific system volume change was defined as $\Delta V = A_0 \delta_p / m$, with δ_p being the piston displacement and m the mass of the silica gel.

III. RESULTS AND DISCUSSION

Through Fig. 1, it can be seen clearly that the nanopore surfaces are lyophobic. As the pressure is relatively low the system response is similar with that of neat liquid, indicating that the liquid phase cannot enter the nanopores. As the pressure is sufficiently high, the liquid overcomes the capillary effect and the pressure induced infiltration takes place. Note that this phenomenon is different from the well known capillary condensation, which happens in lyophilic channels. As the liquid enters the nanopores, the system compressibility increases considerably, resulting in the formation of the infiltration plateau of sorption isotherm. Under quasistatic condition, the infiltration plateau should be perfectly flat if the pore size was uniform. In the system under investigation, because the silica gel exhibits a pore size distribution, the infiltration starts with the largest nanopores at a relatively low pressure and ends with the smallest nanopores at a relatively high pressure. Since the silica gel sample is of a relatively regular nanopore structure,[17] in the following discussion classic Young's equation will be employed to relate the quasistatic infiltration pressure, p_c, to the pore size, D:

$$p_c = \frac{4\Delta\gamma}{D}, \tag{1}$$

where $\Delta\gamma$ is the excess solid-liquid interfacial tension, i.e., the difference between the solid-liquid interfacial tension and the summation of solid and liquid surface tensions. Based on the profiles of infiltration plateaus in Fig. 1, the pore size distribution can be calculated via a Washburn-type analysis,[18] as shown in Fig. 3, with the values of $\Delta\gamma$ being assumed constant and determined by fitting the average pore size to the gas absorption measurement result, $\bar{D}=7.8$ nm. The value of p_c is taken from the sorption isotherm curve of the lowest loading rate, 1 mm/min. Further lowering the loading rate would not cause any detectable changes in infiltration pressure; that is, it can be regarded as quasistatic. Figure 4 shows the excess solid-liquid interface tension, where p_{in} is defined as the infiltration pressure at $\bar{D}$. Note that Eq. (1) is valid only when the loading rate effect is negligible.

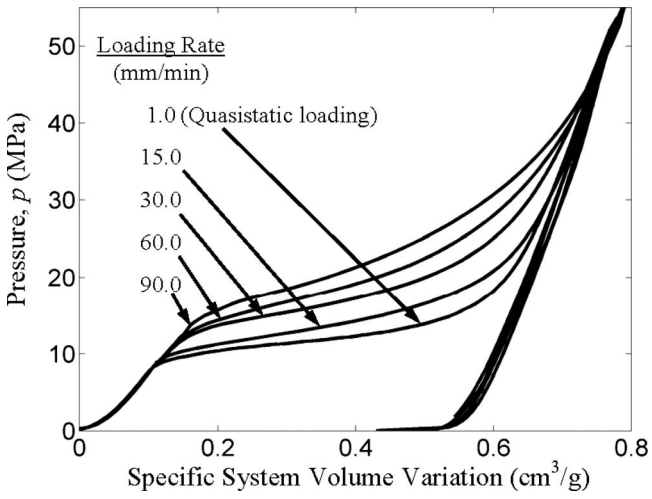

FIG. 2. The loading rate effect on the pure glycerin based system.

The calculated pore size distributions of all the systems are similar to each other, suggesting that in the nanopore size range under investigation, the classic capillary theory can describe the quasistatic liquid infiltration quite well. Moreover, $\Delta\gamma$ is insensitive to the pore size, D. However, at the lower end of pore size range, the pore size distribution data are relatively irregular, which may be attributed to that; as the pore size is comparable with the double layer thickness, the ordinary interface theory is no longer valid and the effective solid-liquid interfacial tension is affected by the confinement effect of pore walls. It may also be related to the influence of the gas phase entrapped in the nanopores, which, when under a high pressure, can dissolve in the confined liquid phase.[19,20] The relationship between the glycerin con-

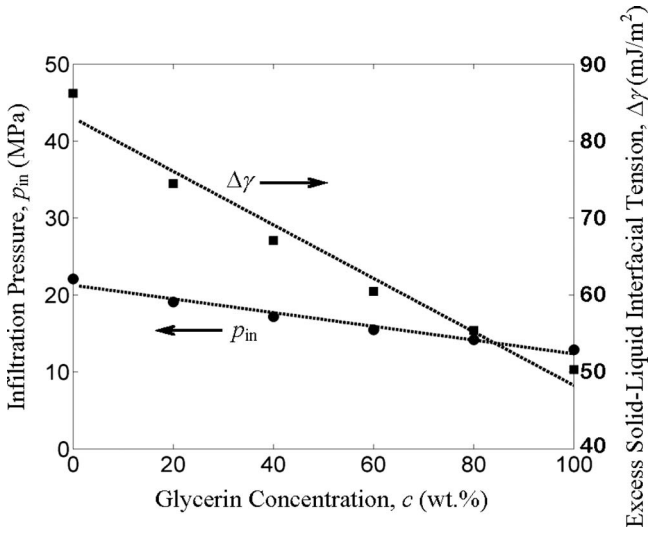

FIG. 4. The infiltration pressure and the excess solid-liquid interfacial tension as functions of the glycerin concentration. The loading rate was 1 mm/min. The nanopore size was 7.8 nm.

centration and p_{in} (or $\Delta\gamma$) is quite linear, suggesting that the effects of different components in the liquid phase can be analyzed by linear superposition.

As the loading rate increases, according to Fig. 2, it is clear that the infiltration pressure of neat glycerin, p, becomes higher; that is,

$$p = p_c + \delta p, \tag{2}$$

where δp is the additional infiltration pressure related to the rate effect. The δp-p_c relation can be obtained by subtracting the quasistatic sorption isotherm curve from the high-loading-rate ones, which, by using Eq. (1), can be converted to the δp-D relation, as shown in Fig. 5. Note that there exists a sharp transition of δp at about 7.3 nm at all the loading rates. In the relatively small nanopores the additional infiltration pressure is higher by about 13 MPa than that in larger nanopores. This value does not vary much as the loading rate increases. The δp-D curve shifts as the loading rate

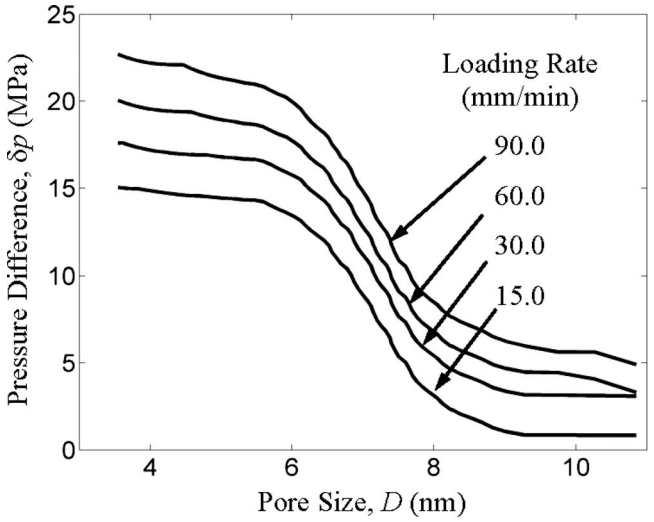

FIG. 5. The increase in infiltration pressure caused by the loading rate effect.

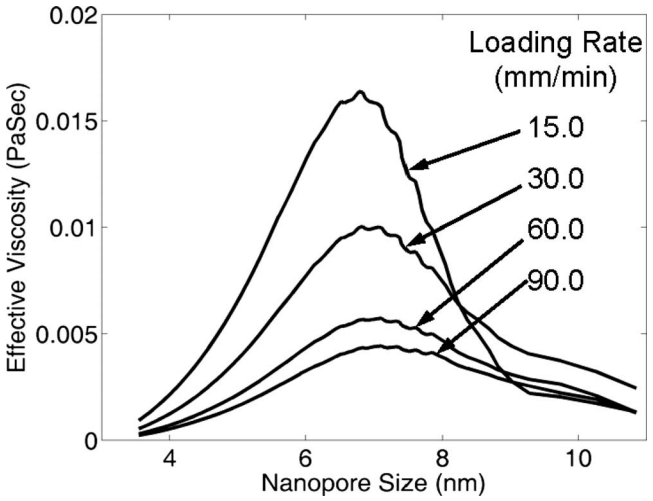

FIG. 6. The effective liquid viscosity as a function of the loading rate and the nanopore size. The system is based on pure glycerin.

varies. That is, when the loading rate becomes higher, the rate effect is more pronounced, as it should be.

Based on the classic circular Poiseuille flow solution,[21] as the first-order approximation, we have

$$\delta p = \frac{128\mu QL}{\pi D^4}, \tag{3}$$

where μ is the effective liquid viscosity in nanopores, Q is the flow rate, and L is the effective nanopore depth. During the infiltration experiment, since the piston speed, v, is constant, the overall flow rate is fixed as vA_0, and the total infiltration time is $t_0 = V_p/vA_0$, with $V_p = 0.28$ cm^3 being the nanopore volume. The time required to fill the nanopores of size D can then be estimated as $t_D = ft_0$, where f is the volume density shown in Fig. 3. Thus, the flow rate in a nanopore can be assessed as

$$Q(D) = (fV_p)/(t_D N) = \pi v A_0 D^2 L/4fV_p,$$

with $N = fV_p/(\pi D^2 L/4)$ being the number of nanopores of size D. Consequently, Eq. (3) can be rewritten as

$$\mu = \alpha \frac{\delta p}{v} D^2 f(D), \tag{4}$$

where $\alpha = V_p/32A_0L^2$. If L is taken as one-half of the average silica particle size, 25 μm, the effective viscosity of glycerin in nanopores can be calculated based on the measurement result of δp, as shown in Fig. 6.

The viscosity of bulk glycerin is 1.49 Pa s.[22] According to Fig. 6, the effective viscosity in nanopores is lower than this value by more than two orders of magnitude. Depending on the pore size and the loading rate, μ varies in the range of 10^{-3}–10^{-2} Pa s. There exists a characteristic nanopore size, D_c, around 7 nm, at which the effective viscosity reaches the maximum value. This characteristic nanopore size slightly increases as the loading rate becomes higher. When the pore size is smaller than D_c, μ decreases with D. At a higher loading rate, the effective μ is smaller. With a constant D, $d\mu/dv$ decreases with the increasing of v; i.e., when v is relatively large, the rate effect on the μ-D curve tends to

saturate. When D is larger than D_c, $d\mu/dD$ is negative and the rate effect is less evident than in smaller nanopores.

The size and rate dependence of the effective viscosity should be associated with the confinement effect of nanopore walls. On the one hand, since the silica surface is lyophobic, it repels liquid molecules, and thus at the solid-liquid interface the density of liquid molecules should be lower. Moreover, the conformation of liquid molecules inside a nanopore is distinct from that of bulk liquid (including the number of nearest neighbors and average spacing), resulting in a different interaction rule. In particular, the fact that after the pressure is reduced to zero no obvious defiltration could be observed (cf. Fig. 1) indicates that the confined liquid molecules are retained at a local energy minimum. Such behavior is often associated with the lost of hydrogen bonds required for infiltration[20] and may cause a smaller viscosity force. Therefore, as the nanopore size is reduced and the solid-liquid interface layer becomes increasingly important, μ tends to decrease. On the other hand, as the nanopore diameter is comparable with the molecular size, across the pore cross section there are only a limited number of molecules, and the continuum theory is no longer valid. For instance, the velocity profile of a Poiseuille flow may not be fully developed. The liquid molecules may move along the nanopore wall. The two competing mechanisms determine the characteristic nanopore size, where the effective viscosity is maximized and the effects of internal friction and liquid density are balanced. When D is relatively small ($D<D_c$), the former mechanism is dominant; when $D>D_c$, the latter is more important. Note that the effective viscosity decreases as the loading rate increases, indicating that the beneficial effect of using viscous liquids for energy absorption under dynamic loadings may be less pronounced than the prediction of continuum fluid mechanics, which is consistent with the experimental results reported by Li.[9]

IV. CONCLUSIONS

In summary, the current study provides experimental results that can be used for theoretical analysis of liquid infiltration in nanoenvironment. The testing data show that under a quasistatic loading, classic Young's equation can capture the infiltration pressure quite well. As liquid composition varies, superposition principle can be employed to analyze the solid-liquid interfacial tension. The effective liquid viscosity is not a material constant; it depends on pore size and loading rate, smaller than its bulk counterpart by two orders of magnitude. There exists a characteristic nanopore size at which the effective viscosity reaches the peak value.

ACKNOWLEDGMENTS

The experiment was supported by the (U.S.) Army Research Office under Grant No. W911NF-05-1-0288. The analysis was supported by the National Science Foundation and the Sandia National Laboratory under Grant No. CMS-0623973.

[1] A. Kalra, S. Garde, and G. Hummer, Proc. Natl. Acad. Sci. U.S.A. **100**, 10175 (2003).
[2] J. C. T. Eijkel and A. van den Berg, Microfluid. Nanofluid. **1**, 249 (2005).
[3] G. Hummer, J. C. Rasaiah, and J. P. Noworyta, Nature (London) **414**, 188 (2001).
[4] R. Z. Wan, J. Y. Li, H. J. Lu, and H. P. Fang, J. Am. Chem. Soc. **127**, 7166 (2005).
[5] S. Sriraman, I. G. Kevrekidis, and G. Hummer, Phys. Rev. Lett. **95**, 130603 (2005).
[6] Y. C. Liu, Q. Wang, L. Zhang, and T. Wu, Langmuir **21**, 12025 (2005).
[7] M. Kruk and M. Jaroniec, Chem. Mater. **13**, 3169 (2001).
[8] S. Polarz and B. Smarsly, J. Nanosci. Nanotechnol. **2**, 581 (2002).
[9] J. C. M. Li, J. Alloys Compd. **310**, 24 (2000).
[10] V. D. Borman, A. A. Belogorlov, A. M. Grekhov, G. V. Lisichkin, V. N. Tronin, and V. I. Troyan, J. Exp. Theor. Phys. **100**, 385 (2005).
[11] X. Kong, F. B. Surani, and Y. Qiao, J. Mater. Res. **20**, 1042 (2005).
[12] X. Kong and Y. Qiao, Philos. Mag. Lett. **85**, 331 (2005).
[13] X. Kong and Y. Qiao, Appl. Phys. Lett. **86**, 151919 (2005).
[14] F. B. Surani, X. Kong, D. B. Panchal, and Y. Qiao, Appl. Phys. Lett. **87**, 163111 (2005).
[15] A. Han and Y. Qiao, J. Phys. D **40**, 5743 (2007).
[16] M. Kumar and P. N. Shankar, Proc. R. Soc. London **444**, 573 (1994).
[17] O. Terasaki, T. Ohsuna, Z. Liu *et al.*, Stud. Surf. Sci. Catal. **141**, 27 (2002).
[18] J. C. Giddings, *Unified Separation Science* (Wiley, New York, 1991).
[19] F. B. Surani and Y. Qiao, J. Appl. Phys. **100**, 034311 (2006).
[20] Y. Qiao, G. Cao, and X. Chen, J. Am. Chem. Soc. **129**, 2355 (2007).
[21] J. A. Fay, *Introduction to Fluid Mechanics* (MIT, Cambridge, MA, 1994).
[22] F. M. White, *Viscous Fluid Flow* (McGraw-Hill, New York, 2005).